Electronic Supplementary Information

Super-Resolution Imaging of Linearized Chromatin in Tunable Nanochannels

Ji-Hoon Lee,[†a,b] Joyce Han-Ching Chiu,[†a,b] Nicholas J. Ginga,[c] Tasdiq Ahmed,[a,b] M. D. Thouless,[d] Yifan Liu,[*e] and Shuichi Takayama[*a,b]

[a] Wallace H. Coulter Department of Biomedical Engineering, Georgia Institute of Technology and Emory University School of Medicine, Atlanta, GA 30332, USA

[b] The Parker H. Petit Institute of Bioengineering and Bioscience, Georgia Institute of Technology, Atlanta, GA 30332, USA

[c] Department of Mechanical and Aerospace Engineering, University of Alabama in Huntsville, Huntsville, AL 35899, USA

[d] Department of Mechanical Engineering and Department of Materials Science and Engineering, University of Michigan, Ann Arbor, MI 48109, USA

[e] Department of Biochemistry and Molecular Medicine, University of Southern California Keck School of Medicine, Los Angeles, CA 90033, USA.

†Contributed equally

*E-mails: yliu3636@usc.edu, takayama@gatech.edu

KEYWORDS: h-PDMS, chromatin linearization, super-resolution imaging, dSTORM

Oxidized-PDMS to optimize multi-color dSTORM imaging

To perform multi-color dSTORM imaging of molecules trapped within completely collapsed (i.e., fully-closed) nanochannels, we first needed to recreate such an environment and optimize dye selections accordingly. Unlike the h-PDMS nanochannels, oxidized-PDMS (ox-PDMS) nanochannels often form pockets containing liquid bubbles when the channels are closed.[1] Therefore, we separately fabricated (**Figure S1**) ox-PDMS devices, and then trapped a panel of fluorophores (in differing buffers) in the fluid pockets of the ox-PDMS nanochannels.

The fluid pockets were first verified with a standard epi-fluorescent microscope before transferring to the dSTORM system. As expected, imaging Alexa Fluor 647 (AF647) and CF568 in conventional GluOx based imaging buffer (BB) was inoperable (**Figures 4B-C**). The reducing agents were not able to overcome the oxygen-rich environment and could not revert the fluorophores back into their dark triplet state, the fluorophores, therefore, bleached out under less than a hundred frames of acquisitions. Oxygen scavenging solution, OxEA, was mixed with imaging buffer in an attempt to remove oxygen diffused into the surrounding PDMS. Photo-blinking with AF and CF dyes were observed (**Figures 4D-E**). However, compared to an ideal situation where AF and CF dyes are exposed to the copious amount of imaging buffer or OxEA solution, photo-bleaching was still significant. Approximately five hundred frames were collected before the dyes were no longer able to switch between their dark and fluorescent states. This was a much lower number of acquisition frames compared to the thousands of frames customary of super-resolution imaging procedures. The amount of oxygen removed was insufficient via the OxEA method. The sub-optimal effectiveness was hypothesized to be affected by the extremely small dimensions of nanochannels in their closed state. Only a minute quantity of fluorophores was exposed to the imaging or OxEA buffer, thereby resulting in

insufficient quenching. From the optimization experiment, we selected appropriate dyes and buffers for the multi-color imaging of linearized chromatin fibers (**Table S4**).

Uneven BrdU along linearized chromatin fibers

It was evident from analyzing the linearized chromatin fibers that the BrdU was unevenly distributed in the two halves along the linearized rDNA chromatin fibers (**Table S4**). While the true BrdU distributions would be even across the two halves, the observed deviation from this expectation is predominantly due to the limited detection of BrdU. BrdU epitopes are sequestered away from anti-BrdU antibodies, hence limiting detection sensitivity. Moreover, It is for this reason click chemistry is often the preferred method of labeling DNA.[2] Nevertheless, we were able to confirm the segregation patterns of histones, which was the focus of our study.

Detailed h-PDMS device fabrication protocol

Below is the detailed protocol for h-PDMS device fabrication:

1) Add the following into a scintillation vial in sequence, 1.7 g of (7.0-8.0% vinylmethylsiloxane) – dimethylsiloxane copolymer, trimethylsiloxy terminated (VDT-731; Gelest Inc.), 9 μL of platinum-divinyltetramethyldisiloxane complex (SIP6831.2, Gelest Inc.) as catalyst, and 12 μL of 2,4,6,8-tetramethyl-tetravinylcyclotetrasiloxane as moderator (396281 Sigma-Aldrich). Thoroughly mix with a vortex mixer for 20 seconds.
2) Add 0.5 g of (25-35% methylhydroxiloxane) – dimethylsiloxane copolymer, trimethylsiloxane terminated (HMS-301; Gelest Inc.). Thoroughly mix for another 20 seconds using a vortex mixer.

3) Dilute the mixture with n-hexane (Optima™ H303-1; FisherSci) to approximately 20% w/w. Vortex for 20 seconds, followed by further homogenization on a shaker for 1 hour.
4) Use a second dilution with n-hexane to obtain very dilute h-PDMS solution (0.5%, 0.75%, 1%, 1.5%, 2%, 4% w/w). Mix well for 20 secs using vortexer and then on a shaker table for 1 hour.
5) Spin coat 2700 μL of the diluted h-PDMS mixture on the silicon SU-8 mold by low speed spin coating. Spin at 100 rpm for 10 seconds with acceleration of 100 rpm/second, followed by 150 rpm for 30 seconds with acceleration of 100 rpm/second.
6) Transfer the h-PDMS coated mold to an oven and cure at 120°C for two minutes.
7) Encase the mold in an aluminum foil holder with the h-PDMS coated surface still exposed to the environment and allow to cool. The purpose of the aluminum foil holder is to contain the liquid PDMS that will be subsequently poured on the mold.
8) Pour 25 g of PDMS (Sylgard 184, Dow Corning) at 5:1 prepolymer to cross-linker ratio on top of the h-PDMS coated mold in the aluminum foil holder.
9) Degas for 10 minutes and then cure at 65°C in an oven for a minimum of 6 hours.

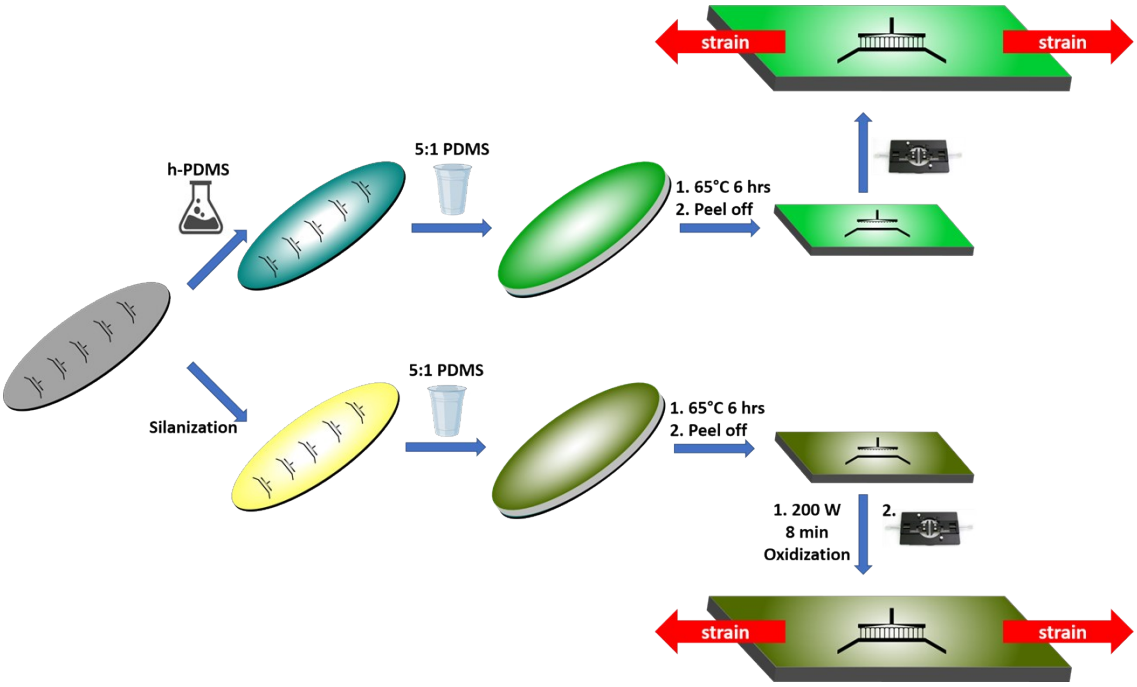

Figure S1. Fabrication processes to create both tunable nanochannels using h-PDMS (top path) and ox-PDMS (bottom path). Desired concentration of h-PDMS was spin-coated on a silicon mold with SU-8 features. Unlike h-PDMS, silanization was required for ox-PDMS. 5:1 PDMS prepolymer-to-crosslinker ratio was used to increase Young's modulus to prevent material failure at the stretcher grips. PDMS was then cured in a 65°C oven for 6 hours. Cracks on h-PDMS were generated using a stretcher, whereas ox-PDMS required plasma oxidization prior to applying strains to initiate cracks.

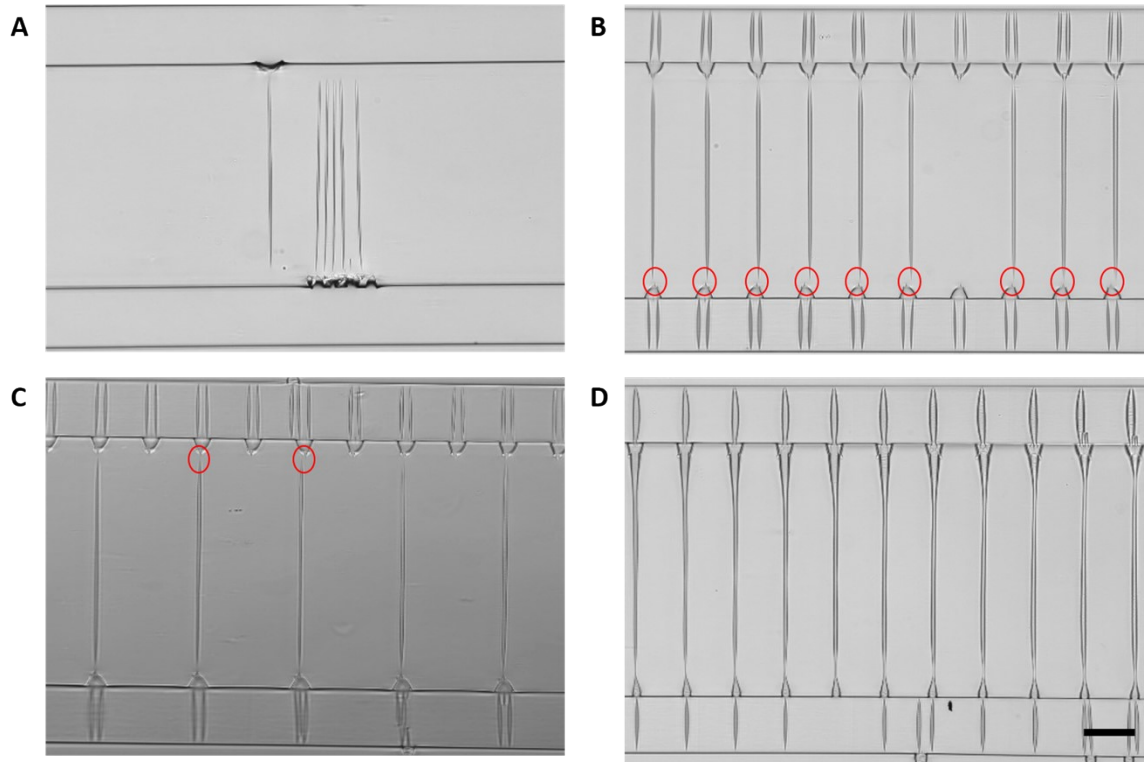

Figure S2. Optical images of top-down view of different v-notch designs to improve control of crack formation. Red circles indicate prematurely terminated cracks. Scale bar = 50 µm. Following the previous work on h-PDMS crack mechanics, v-notches with modified pitch reduced the number of prematurely terminated cracks, irregular and unwanted cracks, and thereby improving device yield. The final device design uses v-notches along only the edge of the inlet microchannel with a 25 µm pitch. (A) Device with no v-notches resulted in stochastic crack generation. (B) Device with equal v-notch spacing along both inlet and outlet microchannels resulting in prematurely terminated cracks. (C) Device with notches along both inlet and outlet microchannels, but with one side having twice the number of notches resulting in prematurely terminated cracks. (D) Device with notches along only the edge of the inlet microchannel resulting in complete crack formation at desired locations.

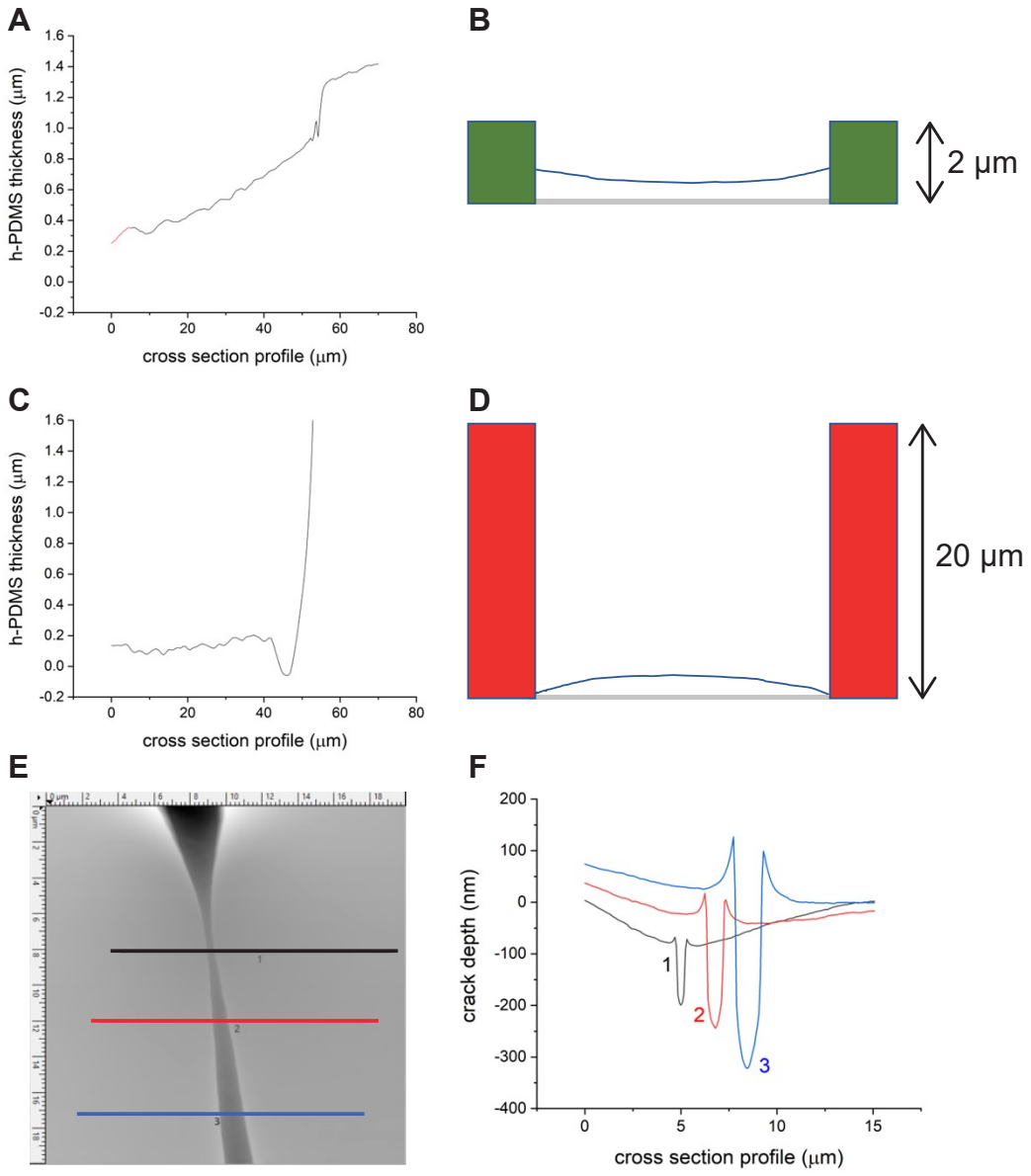

Figure S3. Profilometer measurements revealed that SU-8 thickness of the mold's features affected the thickness profile of the h-PMS film and the subsequent formation of cracks in the film.

Two different h-PDMS thickness profiles were observed between the SU-8 mold features defining the inlet and outlet microchannels. (A) Contact profilometer measurement of h-PDMS and 2-μm-thick SU8 microchannel feature from the midpoint between the inlet and outlet microchannels to one of the SU8 microchannel features. This SU-8 feature thickness resulted in a thicker h-PDMS film near the edge of the inlet and outlet microchannels, and progressively

decreased in thickness towards the midpoint between the inlet and outlet microchannels. (B) Exaggerted schematic representation of convex h-PDMS film distribution generated using 2-µm-thick SU-8. (C) 20-µm-thick SU-8 features caused an opposite h-PDMS film distribution, with its exaggerted schematic representation of concave h-PDMS thickness distribution shown in (D). (E)&(F) Crack depth and crack width measurements using atomic force microscopy at various locations along the length of a crack generated using a 2-µm-thick SU-8 mold.

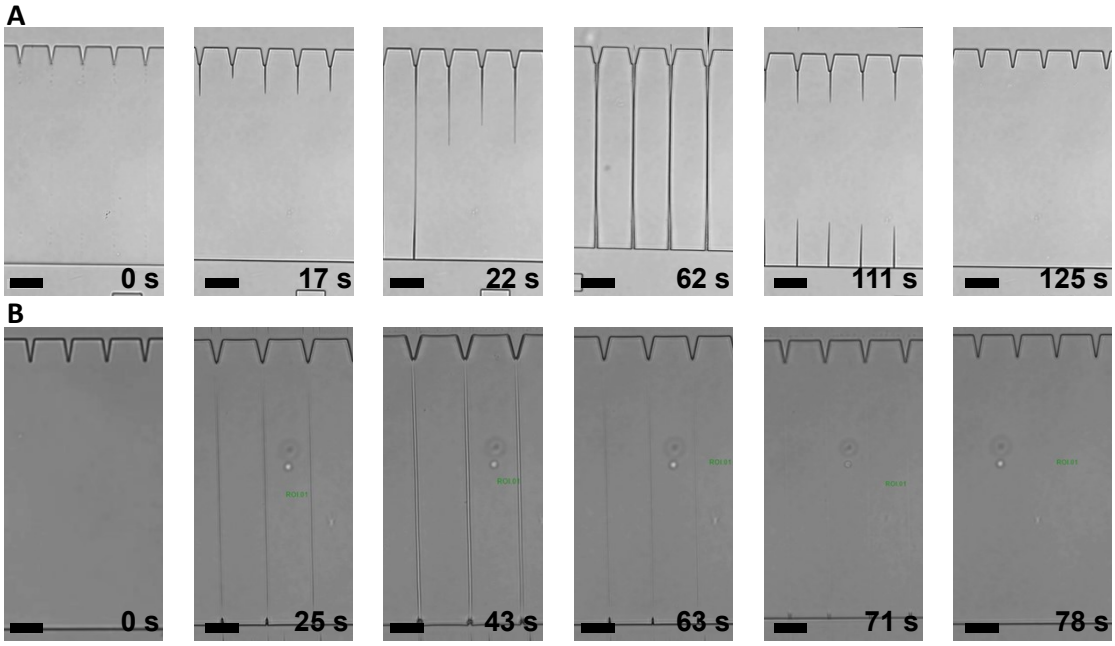

Figure S4. Optical images of top-down view showing contrasting dynamic behaviors of crack opening and closing. (A) The 2-μm-thick SU-8 mold features resulted in an h-PDMS film where the cracks first open at the notches located at the edge of the inlet microchannel and then continue to open unidirectionally toward the other side at the edge of the outlet microchannel. After opening the channels, strain is gradually removed at 111 seconds, and the cracks begin to close. (B) The h-PDMS film produced using the 20-μm-thick SU-8 mold features created cracks that first open at midpoints between the inlet and outlet microchannels and then continue to open bidirectionally towards the inlet and outlet microchannels. After opening the channels, strain is gradually removed at 63 seconds and the cracks begin to close. Scale bars, 50 μm.

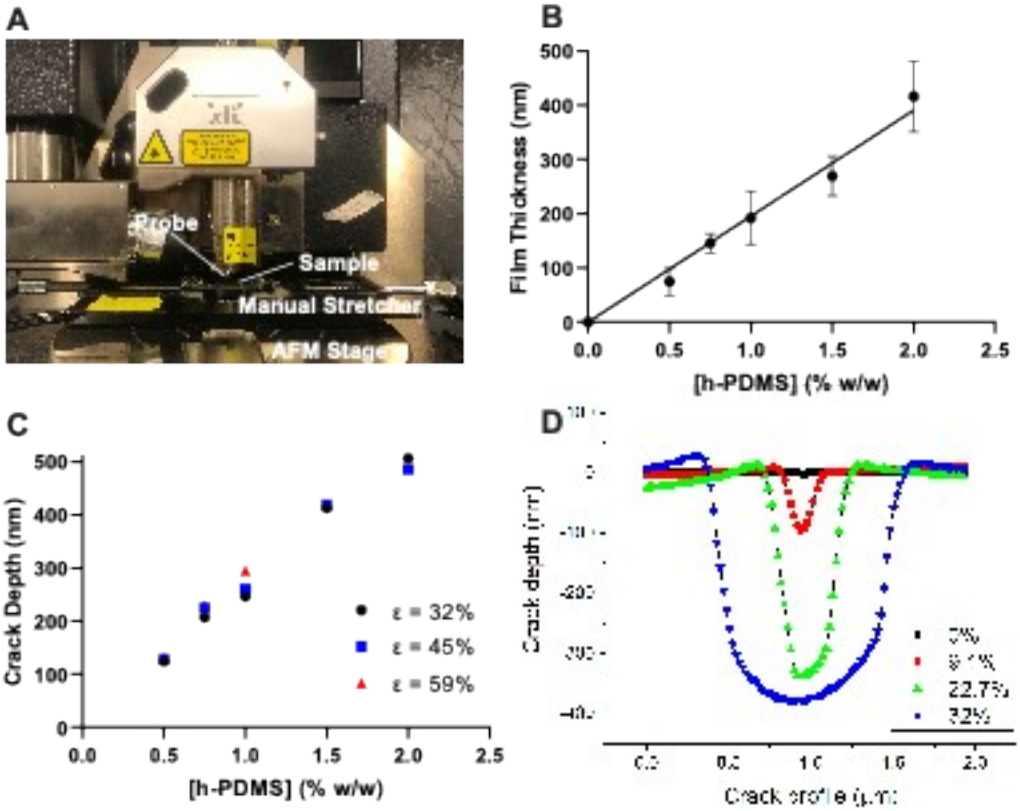

Figure S5. Characterization of h-PDMS film thickness and crack depths. (A) Experimental setup to measure nanocrack profiles using manual stretcher to apply strain to an h-PDMS-PDMS device on an atomic-force microscope. (B) Thickness of h-PDMS layer in nm, *y*, exhibited a linear relationship with the % (*w*/*w*) h-PDMS concentration, *x*. Regression: $y = 195.3x$, $r^2 = 0.984$. (C) AFM measurements of crack depth as a function of % (*w*/*w*) h-PDMS concentrations (i.e. h-PDMS thickness) for various amounts of strain. Given the volume and size contraints for our chromatin linearization application, ~1.5% h-PDMS concentration was selected. (D) AFM measurements of crack profile at various strain values to illustrate crack depth and width when crack is open (32% strain) and closed (0% strain) for a 1.5% h-PDMS film.

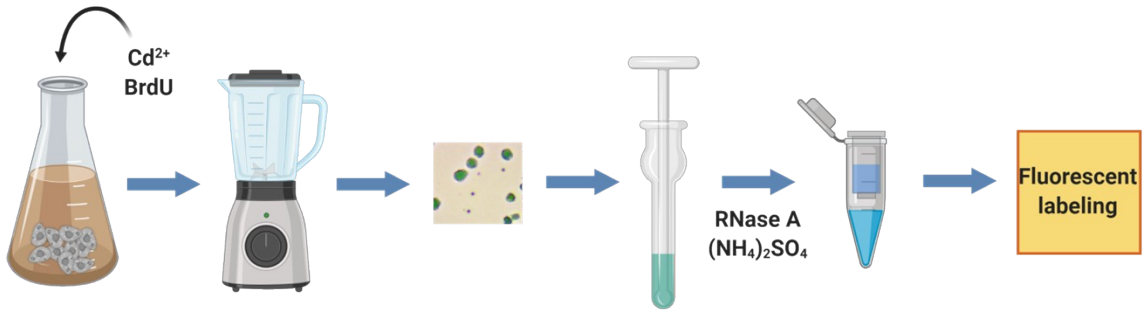

Figure S6. Tetrahymena rDNA extraction procedure. After Tetrahymena were cultured to its logarithmic growth phase, BrdU was introduced to the culture to label new DNA strands for one cell cycle, while cadmium was added to activate HA expression for 1 hour. The cells undergo mechanical lysis with a blender, followed by methyl green verification of nuclei extraction. The nucleoli are extracted with a Dounce homogenizer the resulting solution is treated with RNase and $(NH_4)_2SO_4$ to remove RNA and solubilize non-histone proteins. The extract then underwent multiple wash step for ion exchange and fluorescent labeling to target HA and BrdU.

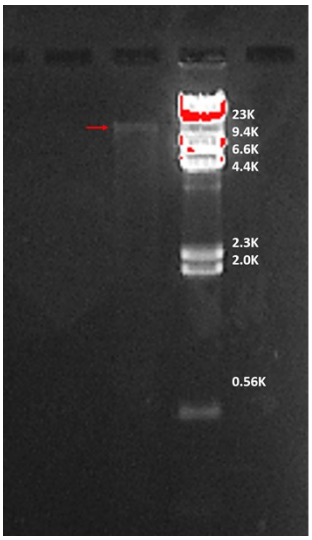

Figure S7. Gel electrophoresis of extracted Tetrahymena rDNA. The assessment was performed in TAE buffer at 100 V and the DNA ladder are from λ-DNA/HindIII Marker (FERSM0101; FisherSci), and successfully verified the 23kb band for rDNA.

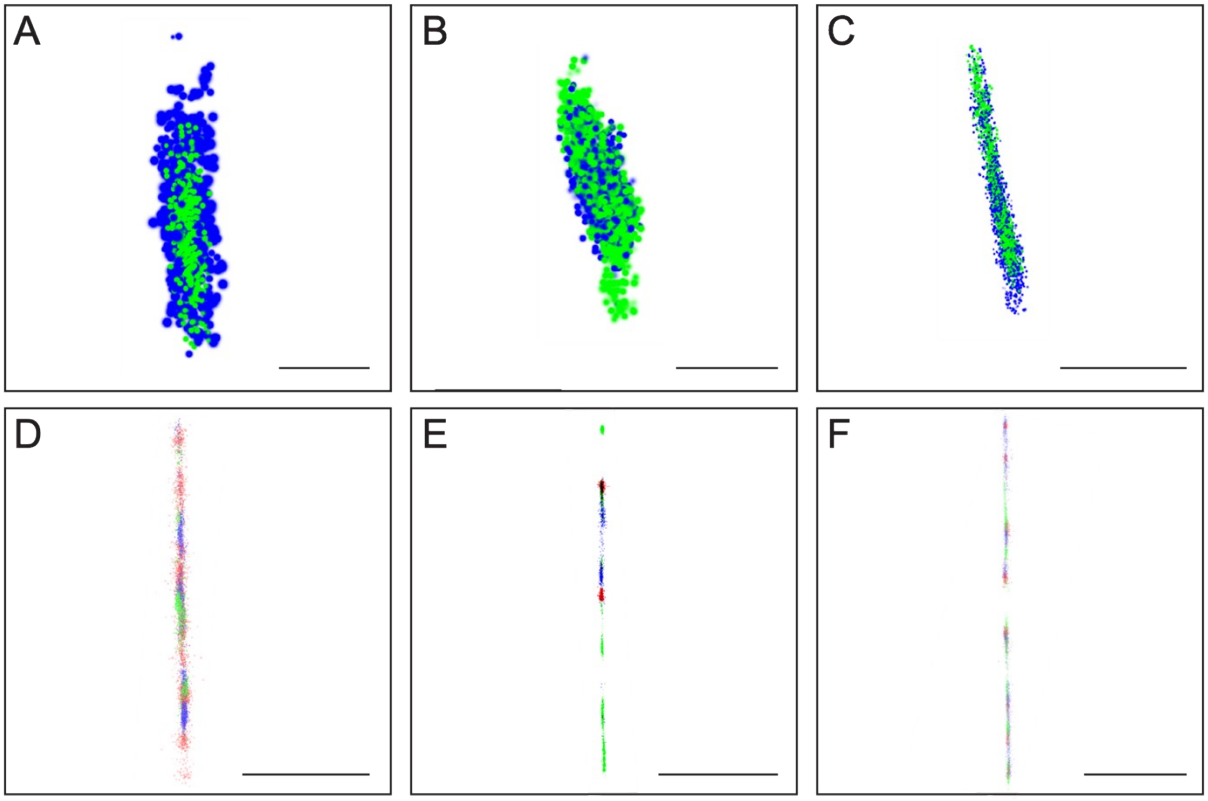

Figure S8. dSTORM images of chromatin fibers that were not considered for analysis. A subset of chromatin fibers was not linearized to its full contour lengths, possibly in the state of random coiled form (A, B, and C). A few were linearized to greater than 150% of the contour length, implying substantial dechromatinization (D, E, and F). Scale bars: 100 nm in (A), 200 nm in (B), 500 nm in (C), 2 μm in (D)-(F).

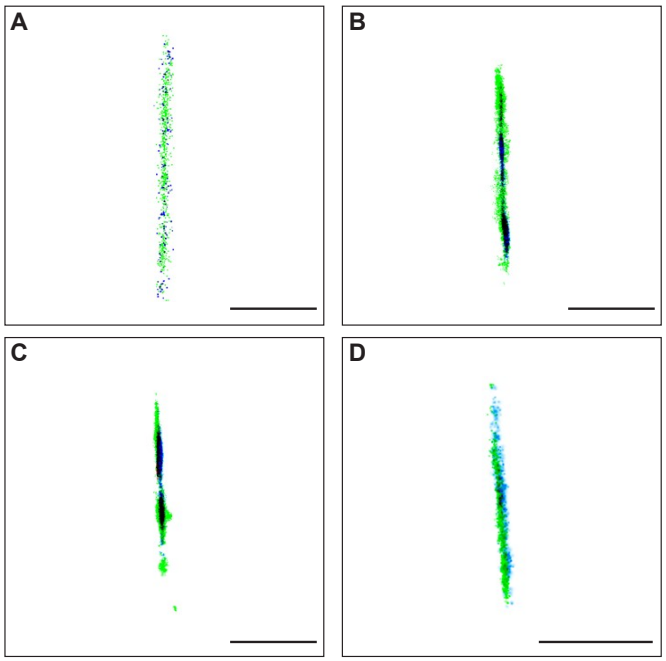

Figure S9. (A)-(D) Additional super-resolution images with random H3 distributions further support dispersive transmission. Scale bar, 1 μm. Green BrDU. Blue H3.

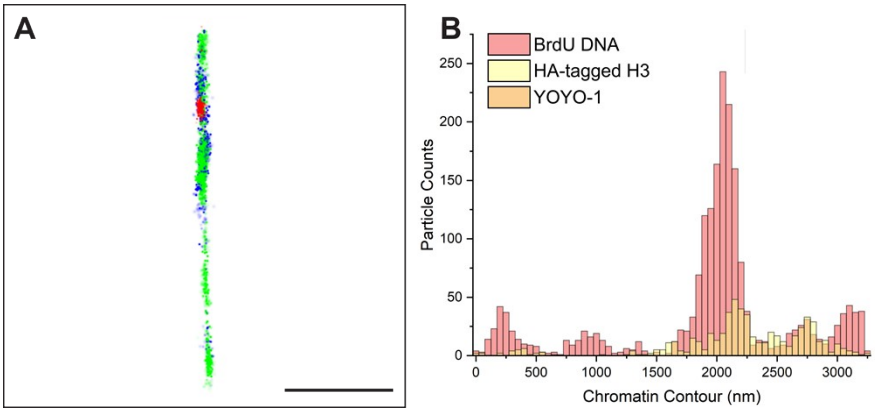

Figure S10. A small subset of results had chromatin fibers with conservative distributions of H3 histones. (A) HA is localized only at the upper half of the linearized fiber. (B) Distribution histogram confirms one-sided H3 histone distribution. Green BrDU. Blue H3. Red YOYO-1

Table S1. Contact angles on features made from the three different SU-8 types.

	SU8-2	SU8-2007	SU8-2025
H_2O	66.9	74.3	83.1
PDMS	30	45.3	51
h-PDMS	27.3	36.6	60.3

Contact angle measurements (in degrees) showed that a progressively hydrophobic behavior (i.e., higher angle) was observed in all three types of solutions. This result suggests that as the dilute h-PDMS solution was spin coated onto the mold, the SU-8 2025 mold would repel h-PDMS more, therefore potentially driving the h-PDMS away from the SU-8 feature. Conversely, the SU8-2 molds would allow easier wetting of the surface, thereby the h-PDMS layer could be more evenly distributed onto the surface. The precise dynamics and spin coating of a thin polymer film is very complex, but here we provide a potential explanation for our observations to why differing distributions of h-PDMS layers are observed with the same deposition method.

Table S2. Summary of crack widths for at different strain levels

hPDMS dilution	ε=32%	ε=45%	ε=59%
0.5%	0.37	0.45	0.46
0.75%	0.56	0.65	0.67
1%	0.725	0.74	1.05
1.5%	1.08	1.26	
2%	1.37	1.48	

The use of an automated stretcher system allowed precise control of strain, hence the crack widths.

Table S3. Summary of crack depths at different strain levels

			Crack Depths (nm)		
hPDMS (%)	**h (nm)**	**stdev (nm)**	**ε=32%**	**ε=45%**	**ε=59%**
0.50%	74.7	25.3	124.8 (50.1)	128.1 (53.4)	130.1 (55.4)
0.75%	145.6	17.58	207.3 (61.7)	225.2 (79.6)	229 (83.4)
1%	192.1	49.2	246.7 (54.6)	260.7 (68.6)	294.8 (102.7)
1.50%	269.5	37	412.7 (143.2)	418.4 (148.9)	NA
2%	415.9	65	506 (90.1)	485 (69.1)	NA

Thickness (h) of h-PDMS layer on a 2-μm-thick SU-8 mold and the corresponding crack depths at approximately 32%, 45%, and 59% strain. The numbers in the parentheses are the differences between the measured h-PDMS thickness and the actual crack depths.

Table S4. Buffers used to optimize imaging in dSTORM

Dye	Buffer	Photobleaching after N frames	Label
AF 647	BB	<100	-
AF 647	OxEA	~500	-
CF 568	BB	<100	-
CF 568	OxEA	~500	-
HMSiR	Water	Thousands	BrdU
FLIP 565	Water	Thousands	HA
HEtetTFER	Water	Thousands	-
CAGE 635	Water	Thousands	-

Optimization of imaging buffers with various dyes was performed. HMSiR and FLIP 565 self-blinking dyes were selected for multi-color imaging of chromatin.

Table S5. Summary of Two-sample Kolmogorov-Smirnov (KS) test results of 6 representative linearized chromatin fibers.

Chromatin	p	Segregation
Figure 6F	0.0925	Dispersive
Figure S9A	0.656	Dispersive
Figure S9B	0.889	Dispersive
Figure S9C	0.0958	Dispersive
Figure S9D	0.0812	Dispersive
Figure S10A	<0.0001	Conservative

Majority of the linearized fibers gave insignifance KS p-values, implying identical distributions between the left and right half of the fibers, thus allowing to categorize the corresponding fibers as 'dispersive' category

References

(1) Matsuoka, T.; Kim, B. C.; Huang, J.; Douville, N. J.; Thouless, M. D.; Takayama, S. Nanoscale Squeezing in Elastomeric Nanochannels for Single Chromatin Linearization. *Nano Lett.* **2012**, *12* (12), 6480–6484. DOI: 10.1021/nl304063f

(2) Salic, A.; Mitchison, T. J. A Chemical Method for Fast and Sensitive Detection of DNA Synthesis in Vivo. *Proc. Natl. Acad. Sci.* **2008**, *105* (7), 2415–2420. DOI: 10.1073/pnas.0712168105.